Nanoscale

Cite this: *Nanoscale*, 2012, **4**, 95

www.rsc.org/nanoscale

COMMUNICATION

Facile synthesis of hierarchical MoS_2 microspheres composed of few-layered nanosheets and their lithium storage properties

Shujiang Ding,[ab] Dongyang Zhang,[a] Jun Song Chen[bc] and Xiong Wen (David) Lou*[bc]

Received 21st October 2011, Accepted 6th November 2011
DOI: 10.1039/c1nr11552a

In this work, we demonstrate an interesting polystyrene microsphere-assisted synthesis of hierarchical MoS_2 spheres composed of ultrathin nanosheets. The as-prepared sample exhibits promising lithium storage properties with improved cyclic capacity retention and rate capability.

As a typical two-dimensional (2D) nanostructure with a large lateral size and a small thickness, nanosheets (NSs) have attracted increasing research interest due to their high surface area, controlled exposed crystal facets,[1–7] diverse compositions such as TiO_2,[1–12] SnO_2[9,13–17] and SnO[18,19] and wide application potentials in many fields such as lithium-ion batteries (LIBs),[1,8–11,13,14,20] gas sensing,[21] glucose sensing[12] and catalysis.[3,5,7,16]

MoS_2 has a similar layered structure with graphite, in which molybdenum atoms are sandwiched between two layers of sulfur atoms. MoS_2 has been found attractive in many applications, such as lubricants,[22] catalysts,[23] and transistors.[24] This layered structure is also beneficial for the intercalation of guest ions, such as Li^+ ions[25–30] and Mg^{2+} ions.[31,32] As a result, many nanostructures of MoS_2 such as nanoflakes, nanotubes and nanoflowers have been reported as electrode materials for LIBs.[29,33,34] Although these MoS_2 nanostructures exhibit high capacities up to 1000 mA h g^{-1}, their cycling stability cannot meet the requirement for practical use in LIBs. Some methods have been proposed to improve the cycling performance of MoS_2 by integrating MoS_2 with different carbonaceous materials, like amorphous carbon, graphene[25,26] and carbon nanotubes (CNTs).[22,35]

Herein, we report a facile synthesis of uniform hierarchically structured MoS_2 microspheres composed of NSs (designated as MoS_2-NS microspheres thereafter), in which polystyrene (PS) microspheres are added to facilitate the assembly of MoS_2 NSs to form uniform microspheres. After an annealing treatment in inert atmosphere, the PS microspheres are decomposed and uniform MoS_2-NS microspheres are obtained. The high surface area resulting from the assembly of nanosheets should help store more lithium ions and the large void space between nanosheets will buffer the volume variation accompanying the charge–discharge process, thus leading to improved cycling stability. As expected, in comparison to MoS_2 flakes, these MoS_2-NS microspheres manifest improved lithium storage properties with better cycling performance and higher capacity.

Fig. 1 shows the morphology of the as-prepared products. From the scanning electron microscopy (SEM; Fig. 1A) image, it is very obvious that the product is composed of PS microspheres and MoS_2-NS microspheres with sizes of ~1.5 μm and ~1 μm, respectively. After being treated in the atmosphere of H_2/N_2 mixture at 800 °C, PS microspheres are decomposed and the MoS_2-NS microspheres are preserved. Fig. 1B shows the morphology of the MoS_2-NS microspheres. It can be seen that these MoS_2-NS microspheres are composed of sheet-like subunits and the size is slightly reduced to 700–900 nm. With a closer examination with transmission electron

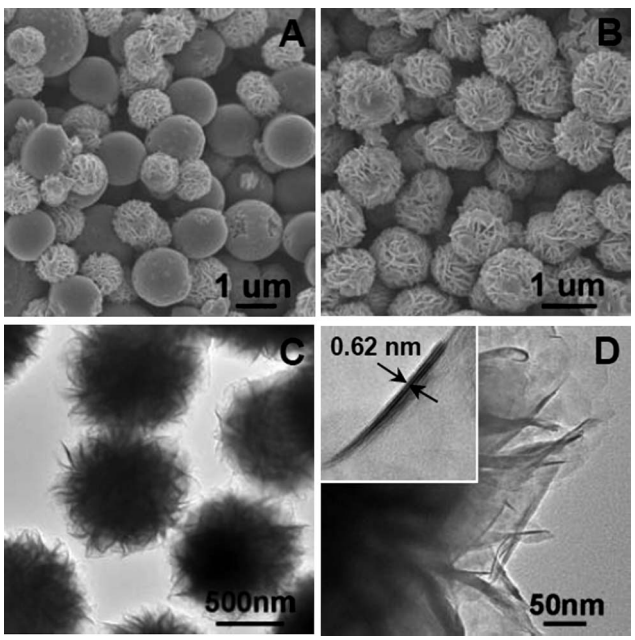

Fig. 1 (A) Scanning electron microscopy image (SEM) of the as-synthesized material; (B) SEM and (C) transmission electron microscopy (TEM) images of the MoS_2-NS microspheres; (D) a high-resolution TEM image of several MoS_2 NSs; the inset shows a HRTEM image of a single MoS_2 nanosheet.

[a]*Department of Applied Chemistry, School of Sciences, Xi'an Jiaotong University, Xi'an, P.R. China 710049. E-mail: dingsj@mail.xjtu.edu.cn*
[b]*School of Chemical and Biomedical Engineering, Nanyang Technological University, 70 Nanyang Drive, Singapore 637457. E-mail: xwlou@ntu.edu.sg*
[c]*Energy Research Institute @ NTU, Nanyang Technological University, 50 Nanyang Drive, Singapore 637553*

microscopy (TEM) (Fig. 1C), the nanosheets with a lateral size of around 500 nm aggregate to form relatively loose microspheres. The high resolution TEM (HRTEM) image (Fig. 1D) shows that the interlayer distance is about 0.62 nm, which is assigned to the (002) plane of MoS_2. The nanosheets are composed of 3–5 layers of MoS_2 molecular sheets.

The crystallinity of the samples is measured by X-ray diffraction (XRD), and the XRD pattern of MoS_2-NS microspheres is shown in Fig. 2A. It is clear that the diffraction peaks at $2\theta = 14$, 33 and 59° can be assigned to (002), (100) and (110) planes of MoS_2 (JCPDS 37-1492) respectively. The surface structure of the MoS_2-NS microspheres is further studied by the gas sorption measurement. From the N_2 adsorption–desorption isotherm (Fig. 2B), a distinct hysteresis loop is identified at a relative pressure of 0.1–0.9, indicating the presence of a mesoporous structure, which leads to a Brunauer–Emmett–Teller (BET) surface area of 36 $m^2\ g^{-1}$. The pore size distribution is calculated by the Barrett–Joyner–Halenda (BJH) method. The plots (inset of Fig. 2B) show that most pores are in the mesoporous range with a peak centered at 3–10 nm. These pores are formed from the stacking of MoS_2 nanosheets.

We have studied the effect of PS on the morphologies of the products. The morphology of the MoS_2 sample prepared by the same hydrothermal route without adding PS is shown in Fig. 3. As can be seen, the MoS_2 product obtained without adding PS is composed of micrometre-sized flakes, which are formed by dense stacking of MoS_2 nanosheets. By comparing the morphologies of MoS_2-NS microspheres and MoS_2 flakes, it is evident that the PS microspheres have played a key role on the formation of MoS_2-NS microspheres. The exact mechanism for the function of PS microspheres is unclear at this moment. It is hypothesized that in the presence of PS microspheres in the solution, nanosheets with smaller thickness and lateral size are formed easily initiated by the functional groups on the PS surface. At the same time, the PS microspheres may act as physical confinement to effectively prevent the further growth of MoS_2 NSs into thick flakes and facilitate the assembly of MoS_2 NSs into microspheres.

Next, we investigate the electrochemical properties of MoS_2-NS microspheres as an anode material for LIBs. Fig. 4A shows the representative cyclic voltammograms (CVs) of MoS_2-NS microspheres. As can be seen, the CV behavior is generally consistent with those reported previously.[25–27,35] In the first cathodic sweep, the peak at 0.74 V is attributed to the intercalation of lithium ions into the MoS_2 lattice which transforms the triangular prism (coordination of Mo by six S atoms) into an octahedral structure.[25,36] This peak

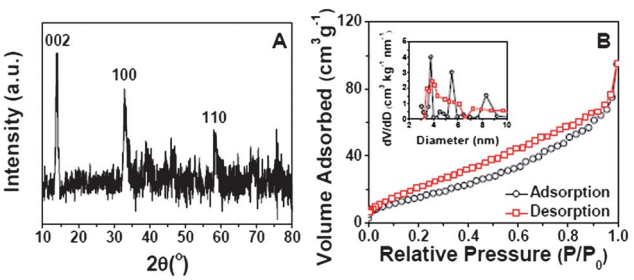

Fig. 2 (A) XRD pattern of MoS_2-NS microspheres; (B) N_2 adsorption–desorption of MoS_2-NS microspheres; the inset shows the pore size distributions calculated from both the adsorption and desorption branches.

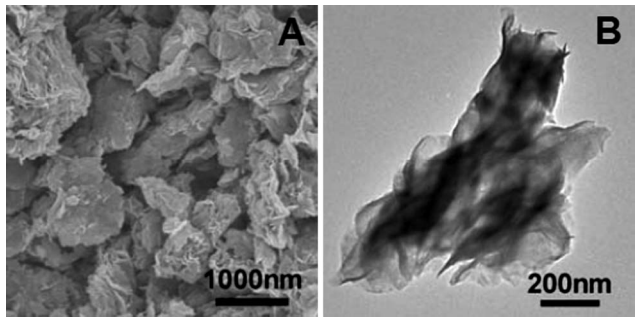

Fig. 3 (A) SEM and (B) TEM images of the MoS_2 flakes obtained without adding PS microspheres.

disappears in the second cathodic sweep because only nearly amorphous MoS_2 is reformed after the charge process (lithium extraction) in the first cycle. The other peak at 0.1 V is attributed to the complete reduction process:[25–27]

$$MoS_2 + 4Li \leftrightarrow Mo + 2Li_2S \quad (1)$$

This peak is shifted to 0.16 V in the second cycle and the current intensity is decreased. In the following cathodic sweeps, two new peaks at 1.8 V and 1.0 V appear, perhaps suggesting the presence of a multi-step lithium insertion mechanism. In the anodic sweeps only one peak at 2.5 V is observed, corresponding to the lithium extraction process and the oxidation of Mo to MoS_2. Fig. 4B shows the charge–discharge voltage profiles of the sample for the first 3 cycles. In agreement with the above CV study, two plateaus at 1.1 and 0.6 V are observed in the first discharge process. The first plateau at 1.1 V is attributed to the formation of Li_xMoS_2, and the plateau at 0.6 V corresponds to the conversion reaction process, in which Li_xMoS_2 is completely decomposed into Mo nanoparticles embedded in a Li_2S matrix and a gel-like polymeric layer is formed resulting from electrochemically driven electrolyte degradation.[25,36] In the second and

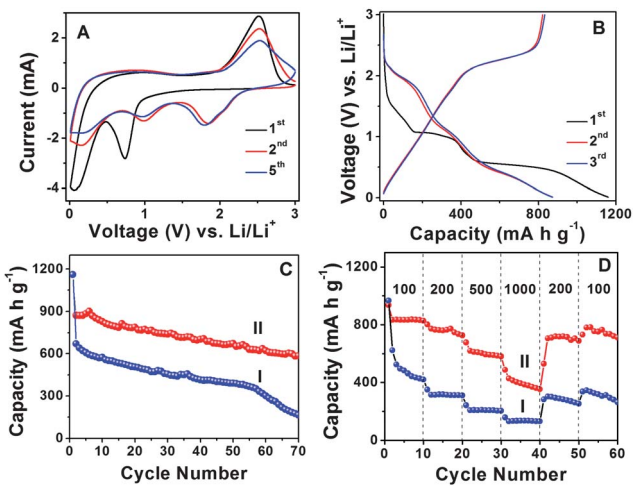

Fig. 4 (A) Representative CVs at a scan rate of 0.5 mV s^{-1} for the first, second, and fifth cycles of MoS_2-NS microspheres. (B) Charge–discharge voltage profiles at a current density of 100 mA g^{-1} of MoS_2-NS microspheres. (C) Comparative cycling performance of MoS_2 flakes (I) and MoS_2-NS microspheres (II) at a current density of 100 mA g^{-1}. (D) Cycling performance of MoS_2 flakes (I) and MoS_2-NS microspheres (II) at different current densities indicated (mA g^{-1}).

third discharge sweeps, the MoS_2-NS microspheres electrode shows two potential plateaus at 1.9 and 1.1 V, and the potential plateau at 0.6 V in the first discharge disappears; in the charge (delithiation) process, the MoS_2-NS microspheres electrode exhibits a conspicuous potential plateau at 2.2–2.4 V, which also agrees with the previous CV curves.

The initial discharge and charge capacities of MoS_2-NS microspheres are found to be 1160 and 791 mA h g^{-1}. Such a high initial lithium storage capacity might be associated with the unique hierarchical structure of the stacked MoS_2 nanosheets. The irreversible capacity loss of around 31.8% may be mainly attributed to the irreversible processes, such as formation of solid–electrolyte interface (SEI) layer and trapping of some lithium in the lattice. The discharge and charge capacities in the second cycle are 873 and 822 mA h g^{-1}, respectively, giving rise to a Coulombic efficiency of 94.2% and this value further increases to 95.4% in the third cycle. Fig. 4C shows the cycling performance at a current density of 100 mA g^{-1}. After 50 discharge–charge cycles, the MoS_2-NS microspheres can still deliver a capacity of 672 mA h g^{-1}, while the MoS_2 flakes only deliver 390 mA h g^{-1}. After 70 cycles, the capacities of MoS_2-NS microspheres and MoS_2 flakes further decrease to 585 mA h g^{-1} and 163 mA h g^{-1}, respectively. Furthermore, the MoS_2-NS microspheres also exhibit better performance compared to the nanocomposite composed of several layered MoS_2 nanosheets on CNTs backbone, whose capacity is about 350 mA h g^{-1} after 50 cycles.[37] Fig. 4D further displays the comparative cycling performance of MoS_2-NS microspheres and MoS_2 flakes at various current densities. At current densities of 200, 500 and 1000 mA g^{-1}, the capacities of MoS_2-NS microspheres are 726, 581 and 353 mA h g^{-1}, respectively as compared to 311, 207 and 134 mA h g^{-1} only for pure MoS_2 flakes. It is thus evident that the MoS_2-NS microspheres exhibit much improved lithium storage performance compared to the pure MoS_2 flakes. The enhanced lithium storage properties might be attributed to the unique hierarchical structure of MoS_2-NS microspheres. Specifically, the large surface area offered by the ultrathin NSs endows the MoS_2-NS microspheres with high specific capacity as a result of increased reactive sites and interface between the active material and electrolyte. Moreover, the presence of sufficient void space between the organized MoS_2 nanosheets not only allows fast lithium ion diffusion but also effectively buffers the mechanical stress and volume variation accompanying the lithium inserting/de-inserting process. Furthermore, the flexible nature of such ultrathin MoS_2 NSs enhances the robustness of the electrode structure.

In summary, we have prepared hierarchical spheres composed of ultrathin MoS_2 nanosheets *via* a facile PS microsphere-assisted hydrothermal method. It is found that the presence of PS microspheres is critical for the formation of such interesting hierarchical spheres. In the absence of PS microspheres, only MoS_2 flakes are formed. Both MoS_2 hierarchical microspheres and flakes have been evaluated as anode materials for lithium-ion batteries. The results show that these unique MoS_2-NS microspheres exhibit greatly enhanced lithium storage properties compared to the MoS_2 flakes.

Experimental section

Materials preparation

In a typical synthesis of MoS_2-NS microspheres, 50 mg of PS microspheres were dispersed into 40 mL of de-ionized water by ultrasonication for 5 minutes. 0.25 g sodium molybdate ($Na_2MoO_4 \cdot 2H_2O$, Sigma-Aldrich) was then added to the above solution. After stirring for 5 minutes, 0.5 g of thiourea was added. After stirring for another 5 minutes, the reaction solution was then transferred to a 60 mL Teflon-lined stainless steel autoclave and kept in an electric oven at 200 °C for 24 h. The autoclave was then left to cool down to room temperature in the oven. The black precipitate was collected by centrifugation, washed thoroughly with ethanol, and dried at 80 °C for 12 h. The as-prepared MoS_2-NS microspheres were further treated at 800 °C in the atmosphere of 5% H_2 balanced by N_2 for 2 h with a heating rate of 1 °C min^{-1} to obtain the highly crystalline MoS_2-NS microspheres. The preparation process of MoS_2 flakes is similar to the one for MoS_2-NS microspheres, except the addition of PS.

Materials characterization

The product morphology was examined using a field-emission scanning electron microscope (FESEM; JEOL, JSM-6700F, 5 kV) and a transmission electron microscope (TEM; JEOL, JEM-2100F, 200 kV). Crystallographic information of the samples was collected using powder X-ray diffraction (XRD; Bruker, D8 Advance X-ray diffractometer, Cu Kα radiation, λ = 1.5406 Å). The nitrogen sorption measurement was performed using a Quantachrome Instrument (Autosorb AS-6B).

Electrochemical measurements

The electrochemical measurements were carried out using two-electrode Swagelok-type cells (X2 Labwares, Singapore) with pure lithium metal as both the counter and the reference electrodes at room temperature. The working electrode consisted of the active material, a conductive agent (carbon black, Super-P-Li), and a polymer binder (poly(vinylidene difluoride), PVDF, Aldrich) in a 70 : 20 : 10 weight ratio. The electrolyte used was 1.0 M $LiPF_6$ in a 50 : 50 (w/w) mixture of ethylene carbonate and diethyl carbonate. Cell assembly was carried out in an Ar-filled glovebox with concentrations of moisture and oxygen below 1.0 ppm. Cyclic voltammetry (0.005–3.0 V, 0.5 mV s^{-1}) was performed using an electrochemical workstation (CHI 660C). The charge/discharge tests were performed using a NEWARE battery tester at different current densities with a voltage window of 0.01–3.0 V.

Notes and references

1 J. S. Chen, Y. L. Tan, C. M. Li, Y. L. Cheah, D. Y. Luan, S. Madhavi, F. Y. C. Boey, L. A. Archer and X. W. Lou, *J. Am. Chem. Soc.*, 2010, **132**, 6124–6130.
2 Y. Q. Dai, C. M. Cobley, J. Zeng, Y. M. Sun and Y. N. Xia, *Nano Lett.*, 2009, **9**, 2455–2459.
3 X. G. Han, Q. Kuang, M. S. Jin, Z. X. Xie and L. S. Zheng, *J. Am. Chem. Soc.*, 2009, **131**, 3152.
4 G. Liu, H. G. Yang, X. W. Wang, L. N. Cheng, J. Pan, G. Q. Lu and H. M. Cheng, *J. Am. Chem. Soc.*, 2009, **131**, 12868–12869.
5 S. W. Liu, J. G. Yu and M. Jaroniec, *J. Am. Chem. Soc.*, 2010, **132**, 11914–11916.
6 H. G. Yang, C. H. Sun, S. Z. Qiao, J. Zou, G. Liu, S. C. Smith, H. M. Cheng and G. Q. Lu, *Nature*, 2008, **453**, 638–641.
7 D. Q. Zhang, G. S. Li, X. F. Yang and J. C. Yu, *Chem. Commun.*, 2009, 4381–4383.
8 J. S. Chen and X. W. Lou, *Electrochem. Commun.*, 2009, **11**, 2332–2335.
9 S. J. Ding, J. S. Chen and X. W. Lou, *Adv. Funct. Mater.*, 2011, **21**, 4120–4125.

10 S. J. Ding, J. S. Chen, D. Y. Luan, F. Y. C. Boey, S. Madhavi and X. W. Lou, *Chem. Commun.*, 2011, **47**, 5780–5782.
11 S. J. Ding, J. S. Chen, Z. Y. Wang, Y. L. Cheah, S. Madhavi, X. Hu and X. W. Lou, *J. Mater. Chem.*, 2011, **21**, 1677–1680.
12 P. Si, S. J. Ding, J. Yu, X. W. Lou and D. H. Kim, *ACS Nano*, 2011, **5**, 7617–7626.
13 S. J. Ding and X. W. Lou, *Nanoscale*, 2011, **3**, 3586–3588.
14 S. J. Ding, D. Y. Luan, F. Y. C. Boey, J. S. Chen and X. W. Lou, *Chem. Commun.*, 2011, **47**, 7155–7157.
15 C. Wang, Y. Zhou, M. Y. Ge, X. B. Xu, Z. L. Zhang and J. Z. Jiang, *J. Am. Chem. Soc.*, 2010, **132**, 46–47.
16 W. W. Wang, Y. J. Zhu and L. X. Yang, *Adv. Funct. Mater.*, 2007, **17**, 59–64.
17 X. M. Yin, C. C. Li, M. Zhang, Q. Y. Hao, S. Liu, L. B. Chen and T. H. Wang, *J. Phys. Chem. C*, 2010, **114**, 8084–8088.
18 B. Kumar, D. H. Lee, S. H. Kim, B. Yang, S. Maeng and S. W. Kim, *J. Phys. Chem. C*, 2010, **114**, 11050–11055.
19 K. Sakaushi, Y. Oaki, H. Uchiyama, E. Hosono, H. S. Zhou and H. Imai, *Small*, 2010, **6**, 776–781.
20 J. H. Chae, K. C. Ng and G. Z. Chen, *Proc. Inst. Mech. Eng., Part A*, 2010, **224**, 479–503.
21 J. H. Lee, *Sens. Actuators, B*, 2009, **140**, 319–336.
22 X. F. Zhang, B. Luster, A. Church, C. Muratore, A. A. Voevodin, P. Kohli, S. Aouadi and S. Talapatra, *ACS Appl. Mater. Interfaces*, 2009, **1**, 735–739.
23 Y. Li, H. Wang, L. Xie, Y. Liang, G. Hong and H. Dai, *J. Am. Chem. Soc.*, 2011, **133**, 7296–7299.
24 B. Radisavljevic, A. Radenovic, J. Brivio, V. Giacometti and A. Kis, *Nat. Nanotechnol.*, 2011, **6**, 147–150.
25 K. Chang and W. Chen, *ACS Nano*, 2011, **5**, 4720–4728.
26 K. Chang and W. X. Chen, *Chem. Commun.*, 2011, **47**, 4252–4254.
27 K. Chang, W. X. Chen, L. Ma, H. Li, H. Li, F. H. Huang, Z. D. Xu, Q. B. Zhang and J. Y. Lee, *J. Mater. Chem.*, 2011, **21**, 6251–6257.
28 G. D. Du, Z. P. Guo, S. Q. Wang, R. Zeng, Z. X. Chen and H. K. Liu, *Chem. Commun.*, 2010, **46**, 1106–1108.
29 C. Q. Feng, J. Ma, H. Li, R. Zeng, Z. P. Guo and H. K. Liu, *Mater. Res. Bull.*, 2009, **44**, 1811–1815.
30 J. Xiao, D. W. Choi, L. Cosimbescu, P. Koech, J. Liu and J. P. Lemmon, *Chem. Mater.*, 2010, **22**, 4522–4524.
31 X. L. Li and Y. D. Li, *J. Phys. Chem. B*, 2004, **108**, 13893–13900.
32 Y. L. Liang, R. J. Feng, S. Q. Yang, H. Ma, J. Liang and J. Chen, *Adv. Mater.*, 2011, **23**, 640–643.
33 H. Li, W. J. Li, L. Ma, W. X. Chen and J. M. Wang, *J. Alloys Compd.*, 2009, **471**, 442–447.
34 R. Dominko, D. Arcon, A. Mrzel, A. Zorko, P. Cevc, P. Venturini, M. Gaberscek, M. Remskar and D. Mihailovic, *Adv. Mater.*, 2002, **14**, 1531–1534.
35 S. J. Ding, J. S. Chen and X. W. Lou, *Chem.–Eur. J.*, 2011, **17**, 13142–13145.
36 Y. Miki, D. Nakazato, H. Ikuta, T. Uchida and M. Wakihara, *J. Power Sources*, 1995, **54**, 508–510.
37 Q. Wang and J. H. Li, *J. Phys. Chem. C*, 2007, **111**, 1675–1682.

